

Linear trinuclear mixed valance Mn^{III} - Mn^{II} - Mn^{III} complex: Synthesis, crystal structure and characterization

Yasemin Yahsi, Elif Gungor, M. Burak Coban & Hulya Kara

To cite this article: Yasemin Yahsi, Elif Gungor, M. Burak Coban & Hulya Kara (2016) Linear trinuclear mixed valance Mn^{III} - Mn^{II} - Mn^{III} complex: Synthesis, crystal structure and characterization, *Molecular Crystals and Liquid Crystals*, 637:1, 67-75, DOI: 10.1080/15421406.2016.1177918

To link to this article: <http://dx.doi.org/10.1080/15421406.2016.1177918>



Published online: 10 Nov 2016.



Submit your article to this journal [↗](#)



Article views: 19



View related articles [↗](#)



View Crossmark data [↗](#)

Linear trinuclear mixed valance $\text{Mn}^{\text{III}}\text{-Mn}^{\text{II}}\text{-Mn}^{\text{III}}$ complex: Synthesis, crystal structure and characterization

Yasemin Yahsi^a, Elif Gungor^a, M. Burak Coban^{a,b}, and Hulya Kara^{a,c}

^aDepartment of Physics, Faculty of Science and Art, Balıkesir University, Balıkesir, Turkey; ^bCenter of Science and Technology Application and Research, Balıkesir University, Balıkesir, Turkey; ^cDepartment of Physics, Faculty of Science, Mugla Sıtkı Koçman University, Mugla, Turkey

ABSTRACT



A new linear trinuclear $\text{Mn}^{\text{III}}\text{-Mn}^{\text{II}}\text{-Mn}^{\text{III}}$ complex **1** has been synthesized and characterized by elemental, spectral, X-ray and magnetic analysis. X-ray diffraction studies show that the central Mn^{II} ion is located at a crystallographic inversion center and is triply bridged to the terminal Mn^{III} ions through one methoxide, one syn-syn carboxylate and one hydroxyl oxygen bridges with the short $\text{Mn}^{\text{III}} \cdots \text{Mn}^{\text{II}}$ distance that is 3.047 Å. The intermolecular C-H \cdots O, C-H $\cdots \pi$ and ring-metal interactions are observed in the hydrogen-bonded assembly of **1**. Magnetic studies reveal that the mixed-valence complex **1** has $S = 3/2$ ground state with antiferromagnetic exchange interactions between Mn^{II} and Mn^{III} ions.

KEYWORDS

Schiff base; mixed-valence Mn complex; X-ray crystal structure; magnetic properties

1. Introduction

Polynuclear manganese complexes continue to attract much attention from groups around the world for its relevance to various areas such as bioinorganic chemistry and molecular nanoscience as well as molecule-based magnet. In the bioinorganic area, the chemistry of high-valent di- or polynuclear manganese complexes is of interest as models for various biological redox-active systems involving Mn ions, such as the oxygen-evolving center (OEC) of photosystem II in green plants in which dioxygen is evolved by water oxidation in photosynthesis, superoxide dismutases, manganese-catalases and manganese ribonucleotide reductase [1]. With regard to the field of molecular magnetism, Mn complexes exhibit the new magnetic phenomenon of single-molecule magnetism (SMM), which is the ability of certain molecules to behave as magnets below a critical temperature exhibiting hysteresis loops in a plot of magnetization versus applied DC magnetic field [2]. Although there are many known species displaying SMM behavior, most of which are manganese-carboxylate complexes [2,3], there is a continuing need for new SMMs. In this context, the carboxylato group is the most extensively studied bridging ligand for its versatility in coordination chemistry and a great number of discrete polynuclear and infinite polymeric manganese-carboxylato complexes with diverse structural motifs and magnetic properties have been reported [4].

CONTACT Yasemin Yahsi  yahsi@balikesir.edu.tr  Department of Physics, Faculty of Science and Art, Balıkesir University, 10145 Balıkesir, Turkey.

Color versions of one or more of the figures in the article can be found online at www.tandfonline.com/gmcl.

© Taylor & Francis Group, LLC

As a result of the above, there continues to be a need to develop new synthetic procedures to polynuclear Mn complexes. Up until now, the structural and magnetic characterization of linear trinuclear Mn^{II} complexes [5] has been published by several research groups where the carboxylate groups act as bridging ligands, but it is interesting to note that little attention has been paid to systems that contain the $\text{Mn}^{\text{III}}\text{-Mn}^{\text{II}}\text{-Mn}^{\text{III}}$ core as shown here [6]. In view of the importance of manganese-carboxylate complexes and our interest in structural and magnetic characterization of manganese complexes [7], we report here the synthesis of a new linear trinuclear mixed valance $\text{Mn}^{\text{III}}\text{-Mn}^{\text{II}}\text{-Mn}^{\text{III}}$ complex along with its single crystal X-ray structure, spectroscopic and also magnetic characterization.

2. Experimental

2.1. Materials and physical measurements

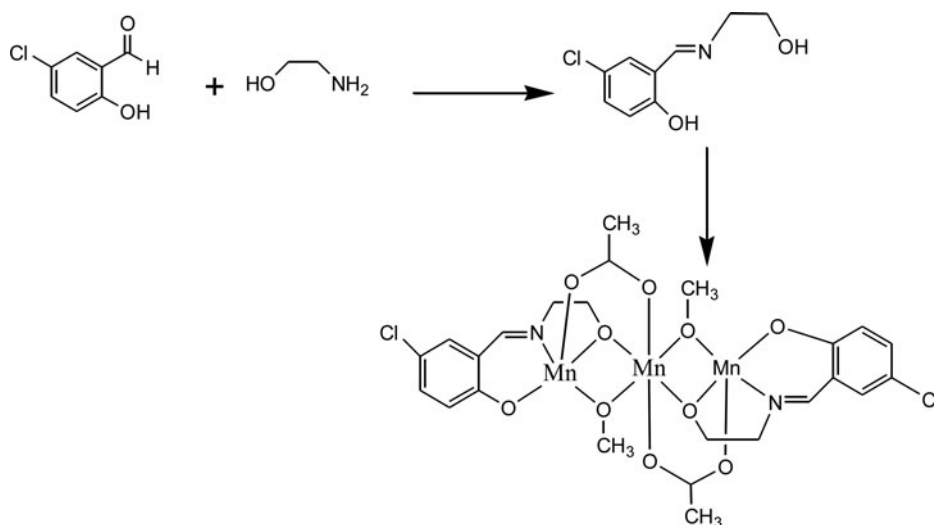
All chemical reagents and solvents were purchased from Merck or Aldrich and used without further purification. Elemental (C, H, N) analyses were carried out by standard methods with an LECO, CHNS-932 analyzer. FT-IR spectra were measured with a Perkin-Elmer Model Bx 1600 instrument with the samples as KBr pellets in the $4000\text{--}400\text{ cm}^{-1}$ range. ^1H and ^{13}C NMR spectra (Figs. S2 and S3) were recorded in (DMSO) on a Bruker Biospin (300 MHz). DC Magnetic measurements were performed using a Cryogenics Squid S600 magnetometer with applied field of 1 T. To avoid possible orientation effects, microcrystalline powders were pressed in pellets. The data were corrected for sample holder contribution and diamagnetism of the sample using Pascal constants. The effective magnetic moments were calculated by the equation $\mu_{\text{eff}} = 2.828 (\chi_{\text{m}} T)^{1/2}$ [8], where χ_{m} , the molar magnetic susceptibility, was set equal to M_{m}/H .

2.2. Synthesis of H_2L

The tridentate Schiff base ligand $\text{H}_2\text{L} = [2\text{-}((E)\text{-}(2\text{-hydroxyethylimino) methyl})\text{-}4\text{-chlorophenol}]$ was synthesized from 5-chlorosalicylaldehyde and ethanolamine in a 1:1 molar ratio in hot ethanol according to the method reported previously [9]. H_2L : Yellow crystals, yield 80%. Anal. Calc. for H_2L : C, 54.15; H, 5.05; N, 7.02. Found: C, 54.11; H, 5.07; N, 7.06%. ^1H NMR (DMSO, δ ppm): 3.74–3.88 (– $\text{NCH}_2\text{CH}_2\text{OH}$, 4H), 5.17 (– $\text{NCH}_2\text{CH}_2\text{OH}$, 1H), 6.69 (– $\text{HC}=\text{COH}$ –, 1H), 7.29 (Cl–C=CH–, 1H), 7.50 (Cl–C–CH–C–, 1H), 8.54 (–HC N–, 1H). ^{13}C NMR (DMSO, δ ppm): 60.83 (–N– CH_2 –), 62.15 (– HOCH_2 –), 119.95 (– $\text{HC}=\text{COH}$ –), 125.90 (C–COH), 127.84 (– $\text{HC}=\text{C}$ –Cl), 130.96 (Cl–C–CH–C–), 132.38 (Cl–C=CH–), 161.45 (–C–COH), 165.91 (–C=N–). IR (KBr) cm^{-1} : ν (O–H) 3165, ν (C=N) 1642.

2.3. Synthesis of complex 1

Complex 1 was prepared by the addition of manganese(II) acetate monohydrate (0.245 g, 1 mmol) in hot methanol (30 cm^3) to the ligand (H_2L) (0.199 g, 1 mmol) in hot methanol (30 cm^3). The mixture has been warmed to 65°C and stirred for 15 min. A green solution was obtained, which was allowed to stand at room temperature for several weeks to afford green crystals. The synthetic route of the complex is outlined in Scheme 1. Complex 1: Yield 75%. Anal. Calc. for $\text{C}_{24}\text{H}_{28}\text{Cl}_2\text{Mn}_3\text{N}_2\text{O}_{10}$: C, 38.94; H, 3.81; N, 3.78. Found: C, 37.80; H, 3.70; N, 3.76%. IR (KBr) cm^{-1} : ν (C=N) 1634.



Scheme 1. The synthetic route of complex **1** evaluated in this study.

2.4. X-ray structure determination

Diffraction measurement was made on a Bruker ApexII kappa CCD diffractometer using graphite monochromated MoK α radiation ($\lambda = 0.71073$ Å) at 100 K. The intensity data were integrated using the APEXII program [10]. Absorption corrections were applied based on equivalent reflections using SADABS [11]. The structure was solved by direct methods and refined using full-matrix least-squares against F^2 using SHELXTL 6.12 [12]. All non-hydrogen atoms were assigned anisotropic displacement parameters and refined without positional constraints. Hydrogen atoms were included in idealized positions with isotropic displacement parameters constrained to 1.5 times the U_{equiv} of their attached carbon atoms for methyl hydrogens, and 1.2 times the U_{equiv} of their attached carbon atoms for all others. The crystal data and structure refinement details for complex **1** are listed in Table 1. Selected bond

Table 1. Crystal data and structure refinement for complex **1**.

Empirical formula	$\text{C}_{24}\text{H}_{28}\text{Cl}_2\text{Mn}_3\text{N}_2\text{O}_{10}$
Formula weight	740.20 g mol $^{-1}$
Temperature	100(2) K
Crystal system	Monoclinic
Space group	$P2_1/c$
Unit cell dimensions	$a = 9.7709$ (3) Å $\alpha = 90^\circ$ $b = 14.9443$ (4) Å $\beta = 91.350$ (2) $^\circ$ $c = 9.6265$ (3) Å $\gamma = 90^\circ$
Volume	1405.26 (7) Å 3
Z	2
Density (calculated)	1405.26 (7) g cm $^{-3}$
Absorption coefficient	1.58 mm $^{-1}$
θ range for data collection	2.1 $^\circ$ to 27.6 $^\circ$
Index ranges	$-12 \leq h \leq 12, -19 \leq k \leq 19, -12 \leq l \leq 12$
Reflections collected	24,043
Independent reflections	3254 [$R_{\text{int}} = 0.055$]
Refinement method	Full-matrix least-squares on F^2
Data/restraints/parameters	2690/0/189
Goodness of fit on F^2	$S = 1.08$
R indices [$I > 2\sigma(I)$]	$R_1 = 0.0312, wR_2 = 0.0728$
Largest diff. peak and hole	0.45 and -0.34 eÅ $^{-3}$

Table 2. Some selected bond lengths [Å] and angles [°] for complex **1**.

Mn1-O1	1.880(2)	Mn2-O2/O2a	2.195(1)
Mn1-O2	1.898(2)	Mn2-O4/O4a	2.178(2)
Mn1-O5	1.879(2)	Mn2-O5/O5a	2.174(2)
Mn1-O3	2.110(2)	Mn1-N1	1.980(2)
O1-Mn1-O2	169.73(7)	O2-Mn2-O2a	180.00(8)
O1-Mn1-O3	94.83(7)	O2-Mn2-O5	71.88(6)
O1-Mn1-O5	97.30(7)	O4-Mn2-O4a	180.00(7)
O1-Mn1-N1	91.45(7)	O4-Mn2-O2a	90.64(6)
O2-Mn1-O3	94.45(7)	O4/O4a-Mn2-O2/O2a	89.36(6)
O2-Mn1-O5	85.51(6)	O5-Mn2-O5a	180.00(8)
O2-Mn1-N1	83.34(7)	O5/O5a-Mn2-O2/O2a	71.88(5)
O3-Mn1-O5	99.39(7)	O5-Mn2-O2a	108.12(5)
O3-Mn1-N1	95.13(7)	O5-Mn2-O4/O4a	90.98(6)
O5-Mn1-N1	162.32(7)	O5/O5a-Mn2-O4/O4a	89.02(6)
Mn1-O2-Mn2	95.97(6)	Mn1-O5-Mn2	97.21(7)

Symmetry code: $a = 1-x, -y, -z$.

lengths and angles for the complex **1** are given in Table 2. A perspective ORTEP view with the atom labeling scheme of complex **1** is shown in Fig. 1 while packing diagrams are given in Fig. 2.

Powder X-ray measurements were performed using $\text{CuK}\alpha$ radiation ($\lambda = 1.5418 \text{ \AA}$) on a Bruker AXS D8 Advance diffractometer equipped with a secondary monochromator. The data were collected in the range $5^\circ < 2\theta < 50^\circ$ in θ - θ mode with a step time of ns ($5 \text{ s} < n < 10 \text{ s}$) and step width of 0.03° .

3. Results and discussion

3.1. Crystal structure description of **1**

The molecular structures of complex **1** consist of neutral linear trinuclear $\text{Mn}^{\text{III}}\text{-Mn}^{\text{II}}\text{-Mn}^{\text{III}}$ [Mn1-Mn2-Mn1a] entity. The central Mn^{II} ion is located at a crystallographic inversion center and is triply bridged to the terminal Mn^{III} ions through one methoxide, one *syn-syn* carboxylate and one hydroxyl oxygen bridges. The terminal Mn^{III} ions are chelated by the tridentate Schiff base ligand by using an imine nitrogen, and phenolate and hydroxyl oxygen atoms. Different Mn-O distances (see Table 2) indicate the complex **1** is in a valence-trapped state. The Mn2-O distances are longest as expected for a lower oxidation state, so we can preliminarily assign Mn2 to Mn^{II} and Mn1 to Mn^{III} ions. Additionally, this can be supported by this that

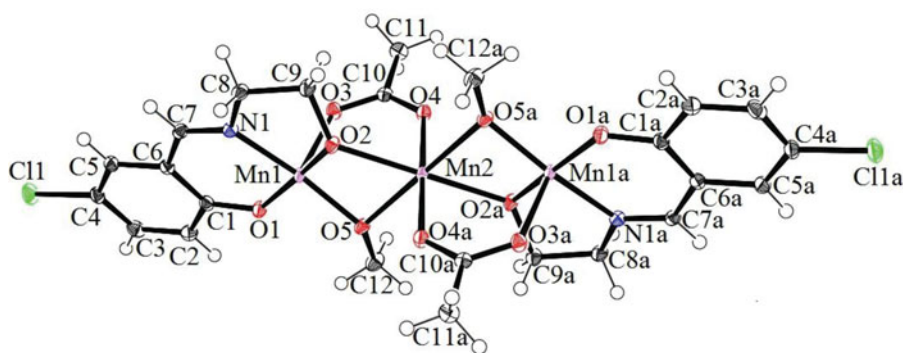


Figure 1. ORTEP drawing of complex **1** with atom labeling. Thermal ellipsoids have been drawn at 50% probability level.

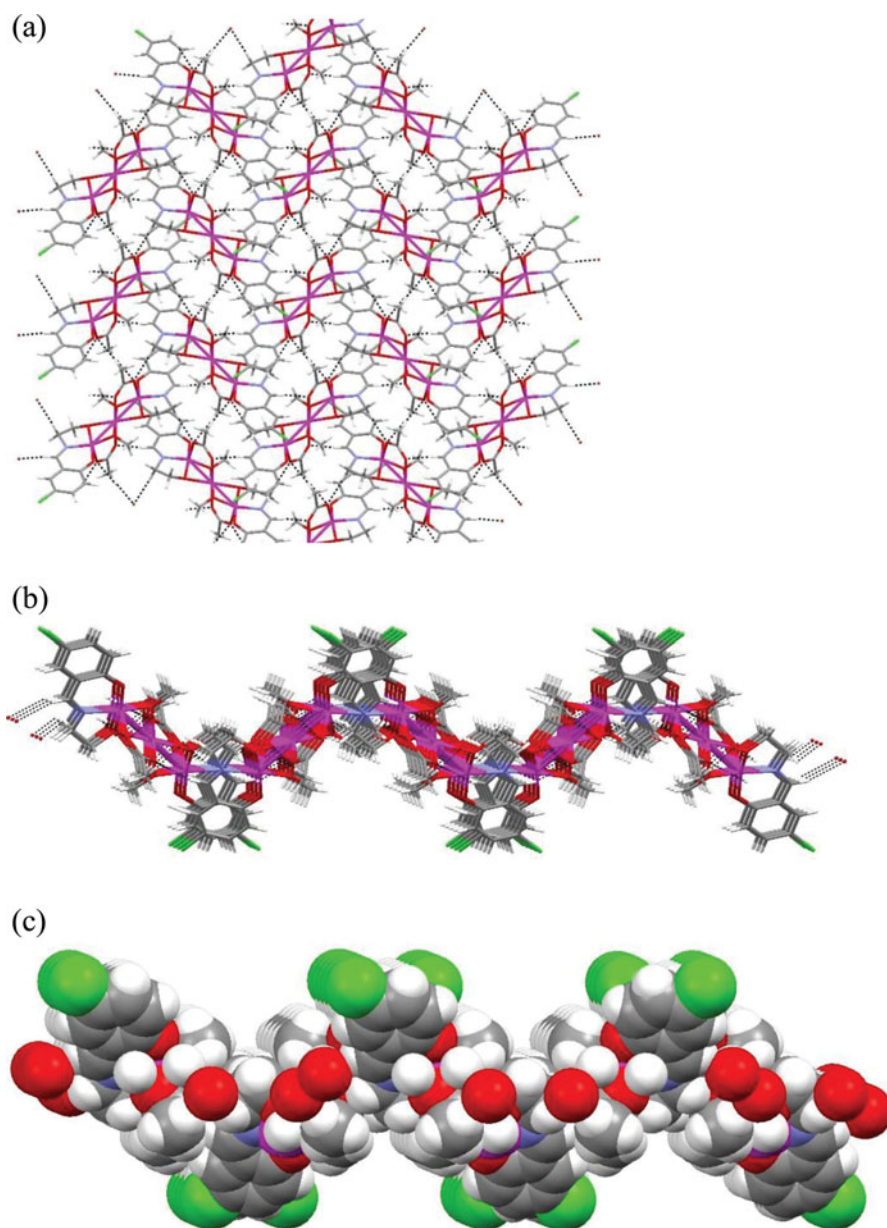


Figure 2. (a) A two-dimensional network structure formed by C-H ...O hydrogen bonds in the *bc*-plane of **1**. (b) View of two-dimensional C-H ...O hydrogen bond found in the crystal structure of **1** along the *c* axis. (c) Space filling representation of **1** as in (b).

Mn-O (-OCH₃) bonds (Mn1-O5 = 1.879 Å and Mn2-O5/O5a = 2.174 Å) are shorter than Mn-O (-CH₃OH) bonds (2.266 Å), which belong to neutral methanol molecule in the literature [6d,6e]. The central Mn^{II} atom (Mn2) is octahedrally coordinated by six oxygen donors with the Mn-O bond distances in the range 2.174(16)-2.195(15) Å (Table 2). Each terminal Mn^{III} atom (Mn1) shows a distorted square-pyramidal environment with four atoms (O1, O2, O5 and N1) in the basal plane and O3 atom in the apical position. For the coordination polyhedron of the metal atom, the distortion of the coordination environment from TBP to SP can be evaluated by the Addison distortion index, τ defined as $\tau = (\alpha - \beta) / 60$, where α and

Table 3. Hydrogen bond geometry (Å, °) and distance between ring centroids [Å] for complex **1**.

<i>D-H...A*</i>	<i>D-H</i>	<i>H...A</i>	<i>D...A</i>	<i>D-H...A</i>	<i>Symmetry</i>
C7-H7...O4	0.95	2.24	3.155	161	1 - x, 1/2 + y, 1/2
C8-H8A...O3	0.99	2.48	3.184	127	x, 1/2 - y, -1/2 + z
C11-H11C...O3	0.98	2.57	3.545	171	1 - x, -y, 1 - z
C12-H12B...Cl1	0.98	2.97	3.62	126	2 - x, 1/2 + y, 1/2 - z
C-H...Cg(I)					
C8-H8A...Cg(4)	0.99	2.73	3.589	146	x, 1/2 - y, -1/2 + z
Cg(I)...Cg(J)					
Cg(4)...Cg(9)			3.627		x, 1/2 - y, -1/2 + z
Cg(I)...Metal					
Cg(9)...Mn1			3.894		x, 1/2 - y, 1/2 + z

*D: Donor, A: Acceptor, Cg(I): Plane number I (= ring number in () above), Cg-Cg: Distance between ring Centroids (Å), Cg-M: Ring-Metal Interactions (Å), Cg(4): -O1-C1-C6-C7-N1 and Cg(9): C1-C2-C3-C4-C5-C6.

β are the two largest coordination angles and $\tau = 0$ for perfect SP and 1 for ideal TBP [13]. The structural distortion indexes of Mn^{III} atom was found $\tau_{\text{Mn1}} = 0.034$. Each Mn^{II} atom is found in a slightly distorted square pyramidal geometry. The Mn1 and Mn2 atoms are in turn associated by O5 and O2 bridges to give chains in the arrangement of {Mn1-Mn2-Mn1a}, and the Mn-O-Mn angles are 97.21(7)° for Mn1-O5-Mn2 and 95.97(6)° for Mn2-O2-Mn1. The intramolecular Mn^{III}-Mn^{II} distance is 3.047 Å. All bond distances and angles are comparable to similar structures [6].

In the crystalline architecture of **1**, intermolecular C-H...O interactions link the molecules that form two-dimensional polymeric structure in the *bc*-plane (Fig. 2(a)). Besides that intermolecular C-H... π and ring-metal interactions are also observed in the hydrogen-bonded assembly of **1** (Table 3).

3.2. IR spectra

The structure of the title complexes were further confirmed by spectral characteristics. The IR spectra of **1** were shown in comparison with that of its free ligand H₂L in Fig. S1. The strong $\nu(\text{O-H})$ (3165 cm⁻¹) band originally found in the Schiff base ligand H₂L disappeared on complexation indicating deprotonation of the phenolic hydroxyl group and coordination of phenolic oxygen to the metal ion. The IR spectra of H₂L show several weak peaks for the complex in the range 2915–2832 cm⁻¹ are likely to be due to the aromatic and aliphatic C-H stretches. The characteristic C=N stretching frequencies are 1634 cm⁻¹. The shift of this band toward lower frequency compared to that of the free Schiff base ligand (1642 cm⁻¹) indicates the coordination of the imine nitrogen atom to the metal center [14]. The strong stretching band appeared at 1493 cm⁻¹ are attributed to the bridging acetate ion [15].

Finally, before proceeding to the magnetic characterization, we note that powder patterns for bulk microcrystalline samples of **1** was consistent with the exclusive presence of the phase identified in the single crystal experiment (Fig. S4 in Supplementary Information).

3.3. Magnetic properties

The magnetic properties of complex **1**, in the form of $\chi_{\text{M}}T$ (χ_{M} is the susceptibility per trinuclear unit) vs. T plots, are shown in Fig. 3 in a temperature range 2–300 K. The $\chi_{\text{M}}T$ values at room temperature, 10 emu K mol⁻¹ ($\mu_{\text{eff}} = 8.95 \mu_{\text{B}}$), which is comparable to the spin-only value of 10.375 emu K mol⁻¹ ($\mu_{\text{eff}} = 9.11 \mu_{\text{B}}$), is expected for three independent

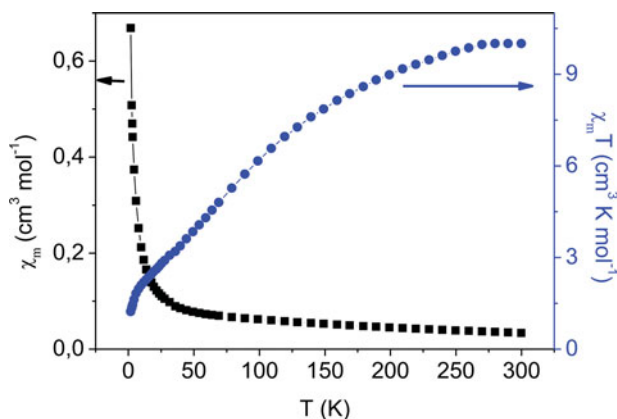


Figure 3. Temperature dependence of χ_m (■) and $\chi_m T$ (•) for **1**.

high-spin Mn ions [$(S_{\text{Mn(III)}}, S_{\text{Mn(II)}}, S_{\text{Mn(III)}}) = (2, 5/2, 2)$ assuming $g = 2.0$]. As the temperature is lowered, the $\chi_m T$ values decrease in a monotonous manner and become $1.23 \text{ emu K mol}^{-1}$ at 1.8 K. This result indicates the presence of an antiferromagnetic spin-exchange interaction between adjacent Mn^{III} and Mn^{II} ions. The drop in the $\chi_m T$ product below 8 K suggests the presence of magnetic anisotropy expected for Mn^{III} ions, inter- or more likely intramolecular antiferromagnetic couplings [16]. The magnetic properties of **1** are comparable for similar trinuclear Mn^{III} , Mn^{II} , Mn^{III} complexes [6a,17].

The magnetic behaviors of **1** are further characterized by field dependences of the molar magnetization at 1.8 K and 4.3 K. The field dependence of the magnetization matches well with the Brillouin function for an $S = 3/2$ ground state with $g = 2$, which would appear as a consequence of the antiferromagnetic interaction through the hydroxyl/ methoxide/carboxylate pathway (Fig. 4). The fact that the magnetization is not fully saturated at high field may be due to the presence of a significant magnetic anisotropy and/or more likely the presence of low-lying excited states that are partially (thermally and field induced) populated [6c].

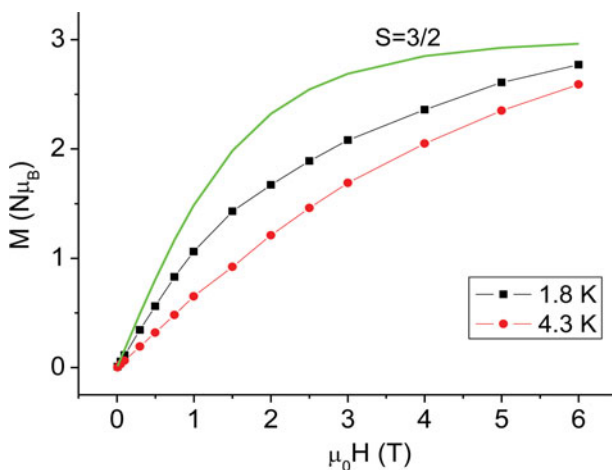


Figure 4. Magnetization as a function of the applied magnetic field for complex **1**, performed at 1.8 K (▲) and 4.3 K (•). The solid line corresponds to the Brillouin function for $S = 3/2$.

4. Conclusions

The synthesis and structural characterization of a new linear trinuclear mixed-valence $\text{Mn}^{\text{III}}\text{-Mn}^{\text{II}}\text{-Mn}^{\text{III}}$ complex has been presented together with an investigation into its magnetic properties. The structurally characterized mixed-valence complex **1** has strictly 180° $\text{Mn}^{\text{III}}\text{-Mn}^{\text{II}}\text{-Mn}^{\text{III}}$ angle as required by crystallographic inversion symmetry. In complex **1**, the exchange interaction between Mn^{II} and Mn^{III} ions is proven to be antiferromagnetic with the spin ground state of $S_T = 3/2$. The prepared complex can be further modified to produce new complexes with higher nuclearity and/or different bridging groups to need for new SMMs and diverse magnetic behavior depending on the structural parameters of the bridging network.

5. Supplementary data

Crystallographic data for the structure reported in this paper have been deposited with the Cambridge Crystallographic Data Centre (The Director, CCDC, 12 Union Road, Cambridge, CB2 1EZ, UK; e-mail: deposit@ccdc.cam.ac.uk; www: <http://www.ccdc.cam.ac.uk>; fax: +44 1223 336033) and are available free of charge on request, quoting the Deposition No. CCDC 826756.

Acknowledgments

The authors are very grateful to Dr. Lorenzo Sorace and Dr. Andrea Caneschi (Department of Chemistry, University of Florence) for the SQUID measurements and helpful suggestions.

Funding

The authors are grateful to the Scientific and Technical Research Council of Turkey (TUBITAK, Grants No. TBAG-108T431) and Balikesir University (Project No. 2015/50) for the financial supports. Dr. Kara also thanks to the Nato-B1-TUBITAK for funding and to Prof. Guy Orpen (School of Chemistry, University of Bristol, UK) for his hospitality.

References

- [1] (a) Pecoraro, V.L. (Ed.) (1992). *Manganese redox enzymes*; VCH Publishers: New York. (b) Christou, G. (1989). *Acc. Chem. Res.*, 22, 328–335. (c) Jiang, W. et al. (2007). *Science*, 316, 1188–1191. (d) Barber, J., & Murray, J.W. (2008). *Coord. Chem. Rev.*, 252, 233–243. (e) Barber, J. (2008). *Inorg. Chem.*, 47, 1700–1710. (f) Tan, Q.H., Wang, Y.Q., Liu, H.T., & Liu, Z.L. (2015). *Inorg. Chem. Comm.*, 58, 67–70. (g) Nitha, L.P., Aswathy, R., Mathews, N.E., Kumari, B.S., & Mohanan, K. (2014). *Spectrochim. Acta Part A*, 118, 154–161. (h) Tu, H.Y., Liu, P., Wang, C.J., Gao, M. X., & Zhang, A.D. (2007). *Mol. Cryst. Liq. Cryst.*, 469, 79–87. (i) Soda, T. et al. (2000). *Mol. Cryst. Liq. Cryst.*, 343, 157–162. (j) Kumagai, H., Markosyan, A., & Inoue, K. (2000). *Mol. Cryst. Liq. Cryst.*, 343, 97–102.
- [2] (a) Gatteschi, D., & Sessoli, R. (2003). *Angew. Chem., Int. Ed.*, 42, 269–297. (b) Christou, G., Gatteschi, D., Hendrickson, D.N., & Sessoli, R. (2000). *MRS Bull.*, 25, 66–71. (c) Aromi, G., & Brechin, E.K. (2006). *Struct. Bond.*, 122, 1. (d) Christou, G. (2005). *Polyhedron*, 24, 2065–2075.
- [3] (a) Stamatatos, T.C. et al. (2005). *J. Am. Chem. Soc.*, 127, 15380–15381. (b) Stamatatos, T.C. et al. (2007). *J. Am. Chem. Soc.*, 129, 9484–9499.
- [4] (a) Rettig, S.J., Thompson, R.C., Trotter, J., & Xia, S. (1999). *Inorg. Chem.*, 38, 1360–1363. (b) Tangoulis, V. et al. (1996). *Inorg. Chem.*, 35, 7655–7660. (c) Colacio, E., Ghazi, M., Kiveka, R., &

- Moreno, J.M. (2000). *Inorg. Chem.*, 39, 2882–2890. (d) Xing-You, X. et al. (2006). *Synth. React. Inorg. Met.-Org. Chem.*, 36, 759–764.
- [5] (a) Kloskowski, M. et al. (2007). *Z. Anorg. Allg. Chem.*, 633, 106–112. (b) Menage, S. et al. (1991). *Inorg. Chem.*, 30, 2666–2671. (c) Lu, X.-M. et al. (2008). *Polyhedron*, 27, 3669–3673. (d) Escuer, A., Cordero, B., Solans, X., Font-Bardia, M., & Calvet, T. (2008). *Eur. J. Inorg. Chem.*, (32), 5082–5087. (e) Rardin, R.L. et al. (1992). *J. Am. Chem. Soc.*, 114, 5240–5249.
- [6] (a) Xie, Q.-W. et al. (2012). *Polyhedron*, 38, 213–217. (b) Li, Y.G., Lecren, L., Wernsdorfer, W., & Clerac, R. (2004). *Inorg. Chem. Comm.*, 7, 1281–1284. (c) Tangoulis, V. et al. (1996). *Inorg. Chem.*, 35, 4974–4983. (d) Thompson, J.R., Ovens, J.S., Williams, V.E., & Leznoff, D.B. (2013). *Chem.-Eur. J.*, 19, 16572–16578. (e) Wu, G. et al. (2013). *J. Am. Chem. Soc.*, 135, 18276–18279.
- [7] (a) Yahsi, Y., & Kara, H. (2014). *Spectrochim. Acta Part A*, 127, 25–31. (b) Yahsi, Y., & Kara, H. (2013). *Inorg. Chim. Acta*, 397, 110–116. (c) Gungor, E., & Kara, H. (2011). *Spectrochim. Acta Part A*, 82, 217–220. (d) Kara, H. (2008). *Anal. Sci.*, 24, x79–80. (f) Kara, H. (2008). *Anal. Sci.*, 24, x263–264. (g) Kara, H. (2008). *Z. Naturforsch.*, 63b, 6–10. (h) Kara, H. (2007). *Z. Naturforsch.*, 62b, 691–695. (i) Karakas, A., Elmali, A., Yahsi, Y., & Kara, H. (2007). *J. Nonlinear Opt. Phys. Mater.*, 16, 505–518.
- [8] Kahn, O. (1993). *Molecular magnetism*; VCHpublishers: New York.
- [9] (a) Gungor, E., Kara, H., Colacio, E., & Mota, A.J. (2014). *Eur. J. Inorg. Chem.*, (9), 1552–1560. (b) Celen, S., Gungor, E., Kara, H., & Azaz, A.D. (2013). *J. Coord. Chem.*, 66, 3170–3181. (c) Gungor, E., Celen, S., Azaz, A.D., & Kara, H. (2012). *Spectrochim. Acta Part A*, 94, 216–221.
- [10] APEX II (version 2010.3-0), Bruker (2010), Bruker-AXS Inc., Madison, Wisconsin, USA.
- [11] SADABS (version 2008/1), Bruker (2008), Bruker AXS Inc., Madison, Wisconsin, USA.
- [12] Sheldrick, G. (2008). *Acta Crystallogr., Sect. A: Found. Crystallogr.*, A64, 112–122.
- [13] (a) Hathaway, B.J., Wilkinson, G., Gillard, R.D., Mc Cleverty, J.A. (Eds.) (1987). *Comprehensive coordination chemistry*, vol. 5, Pergamon Press: Oxford, UK. (b) Addison, A.W., Rao, T.N., Reedijk, J., Rijn, J.V., & Verschoor, G.C. (1984). *J. Chem. Soc. Dalton Trans.*, (7), 1349–1356.
- [14] Horner, O. et al. (1999). *Inorg. Chem.*, 38, 1222–1232.
- [15] (a) Pal, S., Gohdes, J.W., Wilisch, W.C.A., & Armstrong, W.H. (1992). *Inorg. Chem.*, 31, 713–716. (b) Wieghardt, K. et al. (1987). *J. Chem. Soc., Chem. Commun.*, (9), 651–653.
- [16] Mandal, D. et al. (2009). *Inorg. Chem.*, 48, 1826–1835.
- [17] Hanninen, M.M. et al. (2013). *Inorg. Chem.*, 52, 2228–2241.